



Perceived Dark Rim Artifact in First-Pass Myocardial Perfusion Magnetic Resonance Imaging Due to Visual Illusion

Taehoon Shin, PhD^{1, 2}, Krishna S. Nayak, PhD^{3, 4}

¹Division of Mechanical and Biomedical Engineering, Ewha Womans University, Seoul, Korea; ²Department of Medicine, Case Western Reserve University, Cleveland, OH, USA; ³Ming Hsieh Department of Electrical Engineering, University of Southern California, Los Angeles, CA, USA; ⁴Keck School of Medicine, University of Southern California, Los Angeles, CA, USA

Objective: To demonstrate that human visual illusion can contribute to sub-endocardial dark rim artifact in contrast-enhanced myocardial perfusion magnetic resonance images.

Materials and Methods: Numerical phantoms were generated to simulate the first-passage of contrast agent in the heart, and rendered in conventional gray scale as well as in color scale with reduced luminance variation. Cardiac perfusion images were acquired from two healthy volunteers, and were displayed by the same gray and color scales used in the numerical study. Before and after k-space windowing, the left ventricle (LV)-myocardium borders were analyzed visually and quantitatively through intensity profiles perpendicular the borders.

Results: k-space windowing yielded monotonically decreasing signal intensity near the LV-myocardium border in the phantom images, as confirmed by negative finite difference values near the board ranging -1.07 to -0.14. However, the dark band still appears, which is perceived by visual illusion. Dark rim is perceived in the *in-vivo* images after k-space windowing that removed the quantitative signal dip, suggesting that the perceived dark rim is a visual illusion. The perceived dark rim is stronger at peak LV enhancement than the peak myocardial enhancement, due to the larger intensity difference between LV and myocardium. In both numerical phantom and *in-vivo* images, the illusory dark band is not visible in the color map due to reduced luminance variation.

Conclusion: Visual illusion is another potential cause of dark rim artifact in contrast-enhanced myocardial perfusion MRI as demonstrated by illusory rim perceived in the absence of quantitative intensity undershoot.

Keywords: *Dark rim artifact; Visual illusion; Mach band; Myocardial perfusion MRI*

INTRODUCTION

Magnetic resonance (MR) contrast-enhanced myocardial perfusion imaging (MPI) can assess the extent and distribution of ischemia (1-3). In comparison to single-photon emission CT or positron emission tomography, the established methods for clinical evaluation of myocardial perfusion, MR MPI offers superior spatial resolution with

the potential to visualize sub-endocardial defects, and does not involve ionizing radiation. The capability of localizing sub-endocardial defects is of great clinical value since the sub-endocardial layer is the first to be damaged by coronary artery stenosis. Clinical studies evaluating MR MPI have reported high diagnostic sensitivity (88–98%), but relatively low specificity (71–82%), which hampers its widespread clinical use (4-8). This bias is believed

Received June 21, 2019; accepted after revision November 25, 2019.

This work was supported by NRF-2020R1A2C1006293 and NIH R01 HL135500.

Corresponding author: Taehoon Shin, PhD, Division of Mechanical and Biomedical Engineering, Ewha Womans University, 52 Ewhayeodae-gil, Seodaemun-gu, Seoul 03760, Korea.

• Tel: (822) 3277-6534 • Fax: (822) 3277-3535 • E-mail: shinage@gmail.com

This is an Open Access article distributed under the terms of the Creative Commons Attribution Non-Commercial License (<https://creativecommons.org/licenses/by-nc/4.0>) which permits unrestricted non-commercial use, distribution, and reproduction in any medium, provided the original work is properly cited.

to result from the so-called dark rim artifact (DRA) that produces artifactually low signal intensity at the interface between the left ventricle lumen (LV) and the myocardium, potentially leading to a false positive diagnosis (9, 10).

Several potential causes of DRA have been studied to date, but the relative contributions of putative sources remain to be further investigated. Gibbs' ringing has been widely acknowledged as a source of DRA. Due to the truncation by a rectangular window in k-space, intensity difference between LV and the myocardium produces a signal dip right outside the LV. The extent of this signal dip decreases as spatial resolution increases, which motivates the need for the use of high spatial resolution in MPI (9, 11). Cardiac motion is also believed to contribute to the appearance of the DRA. Theoretical and simulation studies using one-dimensional (1D) motion models have confirmed the presence of a dark band along the phase-encoding direction (12, 13). The transient local susceptibility change induced by the contrast agent passage was also believed to contribute to the artifact (14, 15). Ferreira et al. (16) reported a frequency offset ranging from -69 to 85 Hz across the myocardium under typical scan protocols (single dose of contrast agent, 2.4 ms echo time [TE], and 1.5T field strength), which is too weak to cause DRA by intra-voxel dephasing. All of these hypothetical sources can and do contribute to the DRA, complicating its complete analysis.

We present evidence of yet another potential source of perceived DRA, which is associated with a visual illusion caused by the physiology of human visual processing. While the aforementioned sources (Gibbs' ringing, motion, susceptibility) generate a band of quantitatively reduced signal intensity, the artifact induced by the visual illusion is a perceptual phenomenon and related to the way that perfusion images are displayed. The presence of the perceived DRA is demonstrated using numerical phantom and *in-vivo* perfusion data displayed using different color maps.

MATERIALS AND METHODS

Mach Band Illusion

In a mammalian eye, the retinal ganglion cells (RGCs) which constitute the outputs of the retina exhibit a center-surround receptive field structure (17). The excitation of RGC is monotonically related to the difference in light intensity between the center and surround portion of the receptive field. For example, a ganglion cell with an on-center off-surround receptive field structure generates a

vigorous response when a small spot of light is positioned at the center of the receptive field and surrounded by relative darkness (17). If the spotlight area is enlarged to cover both the center and surrounding regions, the cell's spike rate can plummet to levels nearly as low as those measured when there is no light impacting its receptive field. This center-surround response characteristic, often approximated as a Laplacian derivative operator, transmits the difference in light intensity between adjacent regions while remaining relatively insensitive to the actual level of intensity (18). This emphasis in representing contrast over raw intensity in the early stages of visual processing is believed to be responsible for an illusory edge enhancement effect known as the Mach band (19). Mach band appears when two luminance levels are connected by a ramp (Fig. 1). Illusory bright and dark bands are perceived at the two inflection points, despite the absence of a corresponding signal overshoot and undershoot. It should be noted that Mach band is more prominent in achromatic (luminance) contrast than in chromatic contrast (20).

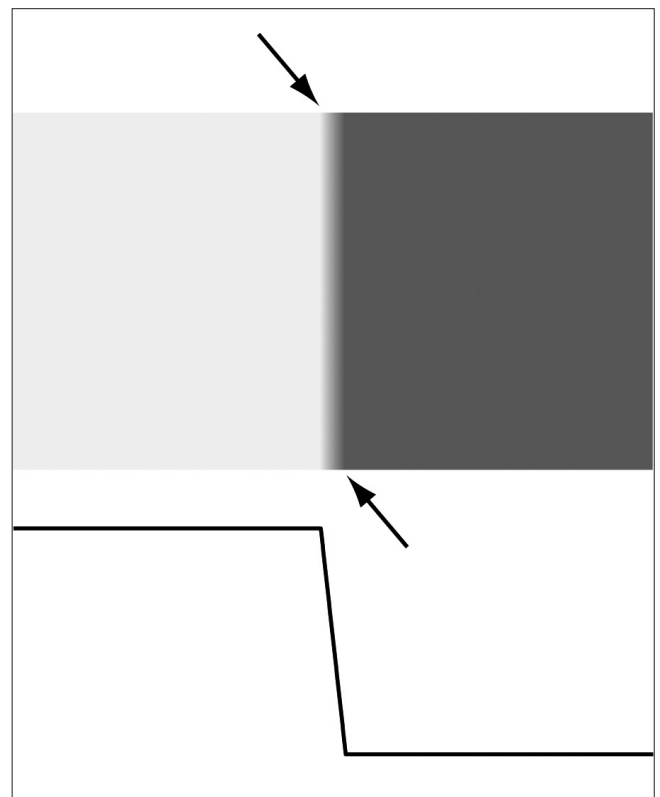


Fig. 1. Illustration of Mach band illusion. Top image presents areas of two intensity levels connected by linear transition. Horizontal intensity profile is shown at bottom. Illusive bright and dark rims are perceived at two inflection points (indicated by arrows), due to contrast enhancement effects in human retina.

Numerical Phantom

Dynamic numerical phantom was used to investigate the perception of the dark rim. The phantom consisted of LV, myocardium, and the right ventricle lumen (RV) with circular or elliptical shapes implemented by corresponding Fourier transforms in k-space. Assuming conditions mimicking cardiac diastolic phase, the phantom had transmural myocardial thickness of 1 cm and spatial resolution of 2.8 mm², which translates to a myocardial thickness of 3.6 pixels. Twenty dynamics were generated to simulate the first pass of a contrast agent from RV through LV and myocardium. Perfusion curves in the three compartments were based on an *in-vivo* first-pass perfusion scan performed in this study. The effect of motion and susceptibility-induced intra-voxel dephasing were excluded from the analysis. The image was 5-fold interpolated by k-space zero-padding to avoid the variability of the dark rim based on the sub-pixel location of LV-myocardium interface (21). Image smoothing was also applied to suppress Gibbs' ringing effect using the Hann windowing in k-space. The window size was adjusted to suppress the actual quantitative signal dip.

The images were rendered either in conventional gray scale or in color scales with reduced luminance variation over the entire intensity range. The luminance of the red, green, blue (RGB) vector can be calculated by an empirical formula (22): 0.3R + 0.59G + 0.11B, which assumes that the mapping between R, G, and B signal levels to the luminance of the output is linear. Two simple color scales were used,

$$[R, G, B] = [x, (0.3 / 0.59)(1 - x), 0] \quad [1]$$

$$[R, G, B] = [x, (0.3 / 0.59)(1 - x), 0.54] \quad [2]$$

where x is normalized image intensity ranging from 0 to 1, with 1 being the highest intensity measured across all time frames. Since the mapping from RGB signal levels to luminance outputs is nonlinear for computer monitors, Equations [1] and [2] often do not result in an iso-luminant chromatic scale. Nevertheless, the resulting color scales exhibit a significantly reduced variation in luminance.

In-vivo Perfusion Images

First-pass perfusion images were acquired from two healthy volunteers (both male, age 41 and 55 years) on a Signa 3T scanner (GE Healthcare, Milwaukee, WI, USA) with an 8-channel cardiac receiver coil. The study protocol was approved by the institutional ethics committee and informed consent was obtained from both participants. The

imaging protocol was designed to minimize the effects of motion and susceptibility changes, leaving Gibbs' ringing as the dominant source of DRA. To minimize motion effects, subjects were instructed to hold their breaths at least until peak myocardial enhancement stage (around 20th cardiac cycle) and data were acquired only during mid-diastole. To reduce susceptibility effects, half of the clinical dose of contrast agent (0.05 mmol/kg) and smallest possible TE (1.0–1.2 ms) were used. The other imaging parameters were $T_{SR} = 120$ ms, repetition time = 2.8–3.2 ms, readout bandwidth = 62.25–125 kHz, flip angle = 12°, spatial resolution = 2.5 × 3.0–3.2 mm², and slice thickness = 8 mm. Rate-2 adaptive sensitivity encoding incorporating temporal filtering (TSENSE) method was used for image reconstruction (23). Perfusion images at 9th (peak LV enhancement), 14th, and 19th (peak myocardium enhancement) cardiac cycles were selected for the analysis of DRA. After sinc interpolation and k-space windowing, the images were displayed on the same gray and color scales used in the numerical phantom study. Six transmural segments perpendicular to the LV-myocardium border were manually selected to investigate the quantitative intensity profiles.

RESULTS

Numerical Phantom

Figure 2 presents the grayscale images of the heart phantom at three representative time frames, before (top row) and after (bottom row) smoothing through k-space windowing. Corresponding signal intensity profiles across the horizontal line at the center are shown at the bottom of each image. The original images prior to smoothing exhibit a dark rim caused by Gibbs' ringing. After k-space windowing, the quantifiable signal dip is removed at all time frames, as validated by the negative finite difference values (i.e., monotonically decreasing) across the LV-myocardium interface, ranging from -1.07 to -0.14. The dark band that appears in the processed image is a Mach band, which is a visual illusion.

The intensity of illusory DRA varies slightly with the spatial position across the myocardium, as well as with the time of acquisition relative to the contrast injection. At peak LV enhancement (Fig. 2D), the dark rim is more intensely perceived around the lateral wall compared to the septal wall, presumably due to larger difference in intensity relative to the neighboring area (background versus RV). The dark rim is less strongly perceived at peak myocardial

enhancement (Fig. 2F) than at the two earlier time frames (Fig. 2D, E), due to smaller difference in intensity between the LV and myocardium. Figure 3 shows the k-space windowed phantom images at the same time frames, but displayed using the two color scales defined as Equations [1] and [2]. The illusory dark band perceived in Figure 2 is eliminated due to the reduced luminance variation in the

color maps used.

In-vivo Perfusion Images

Figure 4 presents illustrative *in-vivo* perfusion images at peak LV enhancement (9th time frame; Fig. 4A, B), myocardial enhancement (19th frame; Fig. 4G, H), and an intermediate time frame (14th frame; Fig. 4D, E). Also

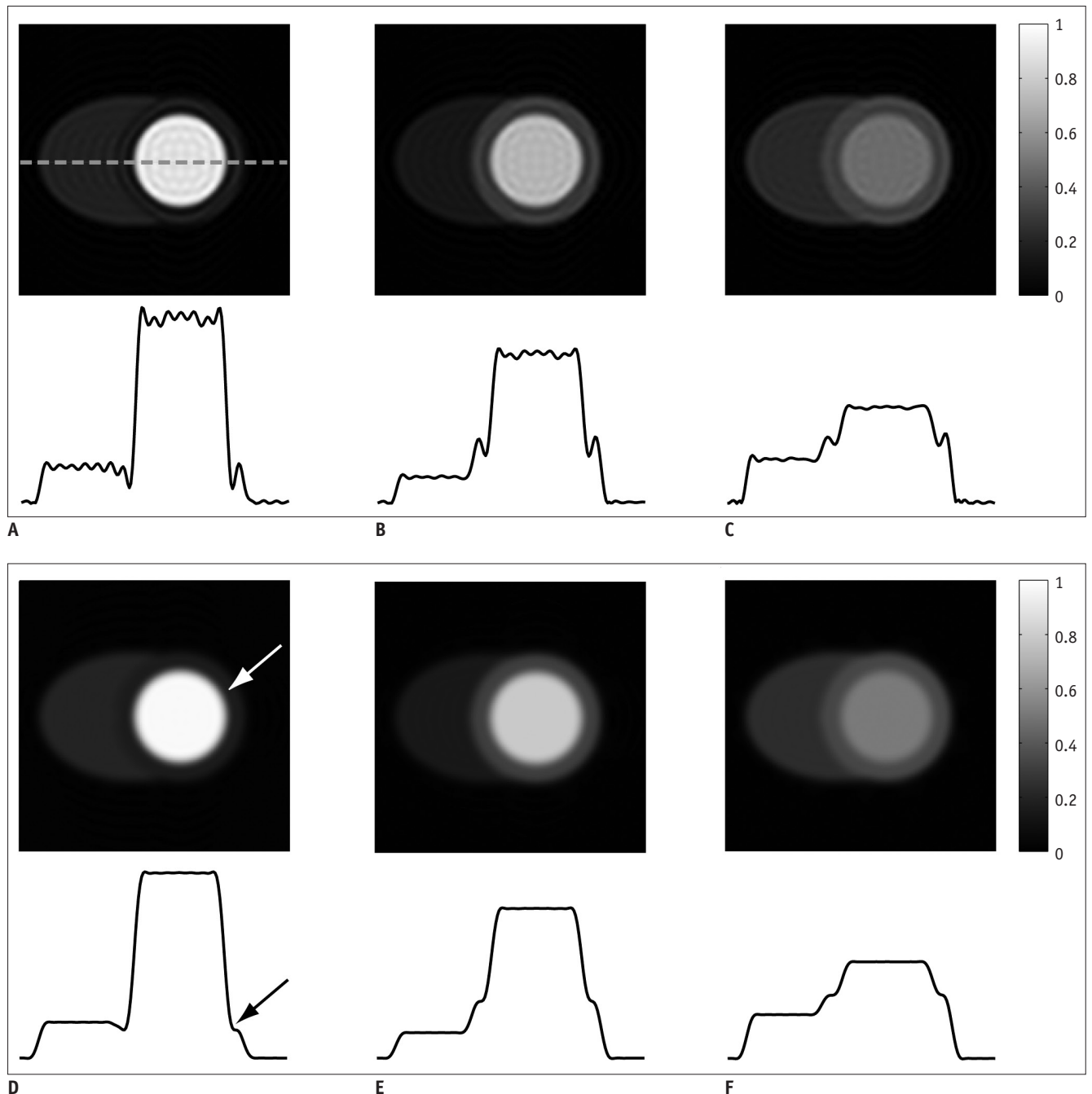


Fig. 2. Grayscale images of heart phantom and one-dimensional intensity profiles along dotted horizontal line. A, D. 9th time frame (peak LV enhancement). B, E. 14th time frame. C, F. 19th time frame (peak myocardium enhancement). Dark rims resulting from Gibbs' ringing are effectively removed by k-space windowing at all three time frames, as validated by intensity profiles. However, dark rim is still visible at all time frames due to Mach band illusion, as indicated by arrows. LV = left ventricle lumen

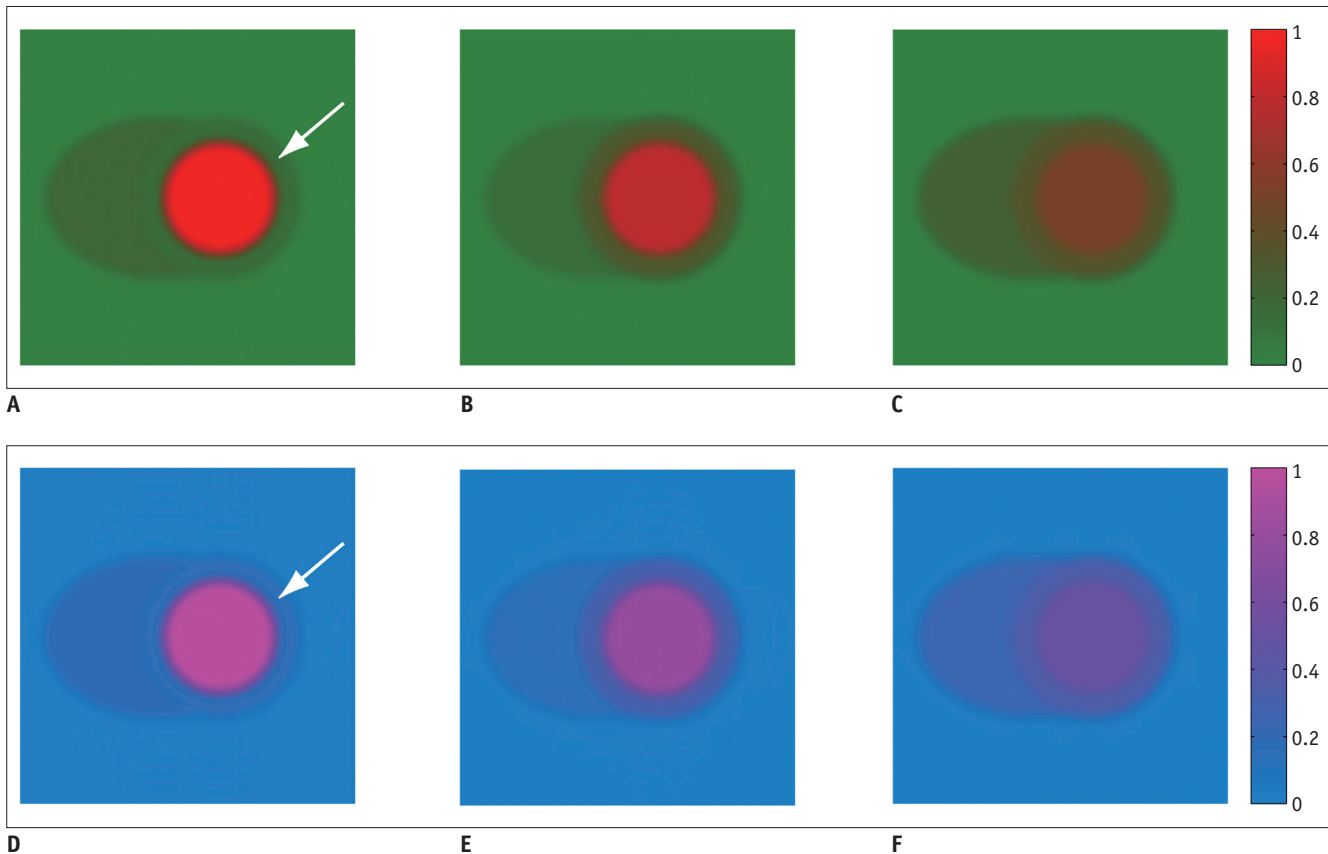


Fig. 3. Color displays of k-space windowed numerical phantom. Two near-isoluminant color scales are used: $[R, G, B] = [x, (0.3 / 0.59)(1 - x), 0]$ (top row), and $[x, (0.3 / 0.59)(1 - x), 0.54]$ (bottom row). **A, D.** 9th time frame. **B, E.** 14th time frame. **C, F.** 19th time frame. Illusory dark rim perceived in Figure 2D-F is eliminated (arrows). This figure was generated using standard International Color Consortium color profile (sRGB IEC61966-2.1), assuming display gamma of 2.2. Appearance of illusory rim may be influenced by display gamma of monitor used to view or printer used to print this manuscript. RGB = red, green, blue

shown are the corresponding intensity profiles across the LV-myocardium interface (Fig. 4C, F, and I, respectively). The original images before smoothing (1st column) exhibit a signal dip at the boundary between LV and myocardium, which is at least partially due to Gibbs' ringing. After smoothing, a dark rim is still perceived along the inferior and lateral walls. However, the corresponding transmural intensity profiles demonstrate effective suppression of the quantitative signal dip, suggesting that the perceived dark rim is a visual illusion. The dark rim is perceived as less intense at the time of peak myocardial enhancement (3rd row) compared to the earlier two time frames (1st and 2nd rows), due to reduced difference in intensity between the LV and myocardium. Figure 5 displays the same images as Figure 4B (Fig. 5A, B) and Figure 4E (Fig. 5C, D) using the same two color scales used in the phantom study, along with corresponding intensity profiles along the six transmural segments (Fig. 5E, F). The illusory dark rim may be notably less intense compared to Figure 4. As a trade-

off, perceived spatial resolution is also reduced.

DISCUSSION

We demonstrate that the perception of DRA can be a result of visual illusion, in addition to other known causes. Numerical heart phantom and *in-vivo* images were shown to exhibit an illusory dark rim in the absence of a quantitative signal dip after image smoothing. While this study has focused on the presence of illusory perception of DRA, it should be noted that there are other known sources of the DRA, including Gibbs' ringing and cardiac motion. All of these causes must be addressed to completely eliminate DRA in first-pass MR MPI.

Approaches to Confirming Illusory DRA

Whether an observed sub-endocardial defect is illusory or true can be determined by quantitatively investigating the intensity profiles in the suspected regions. In this

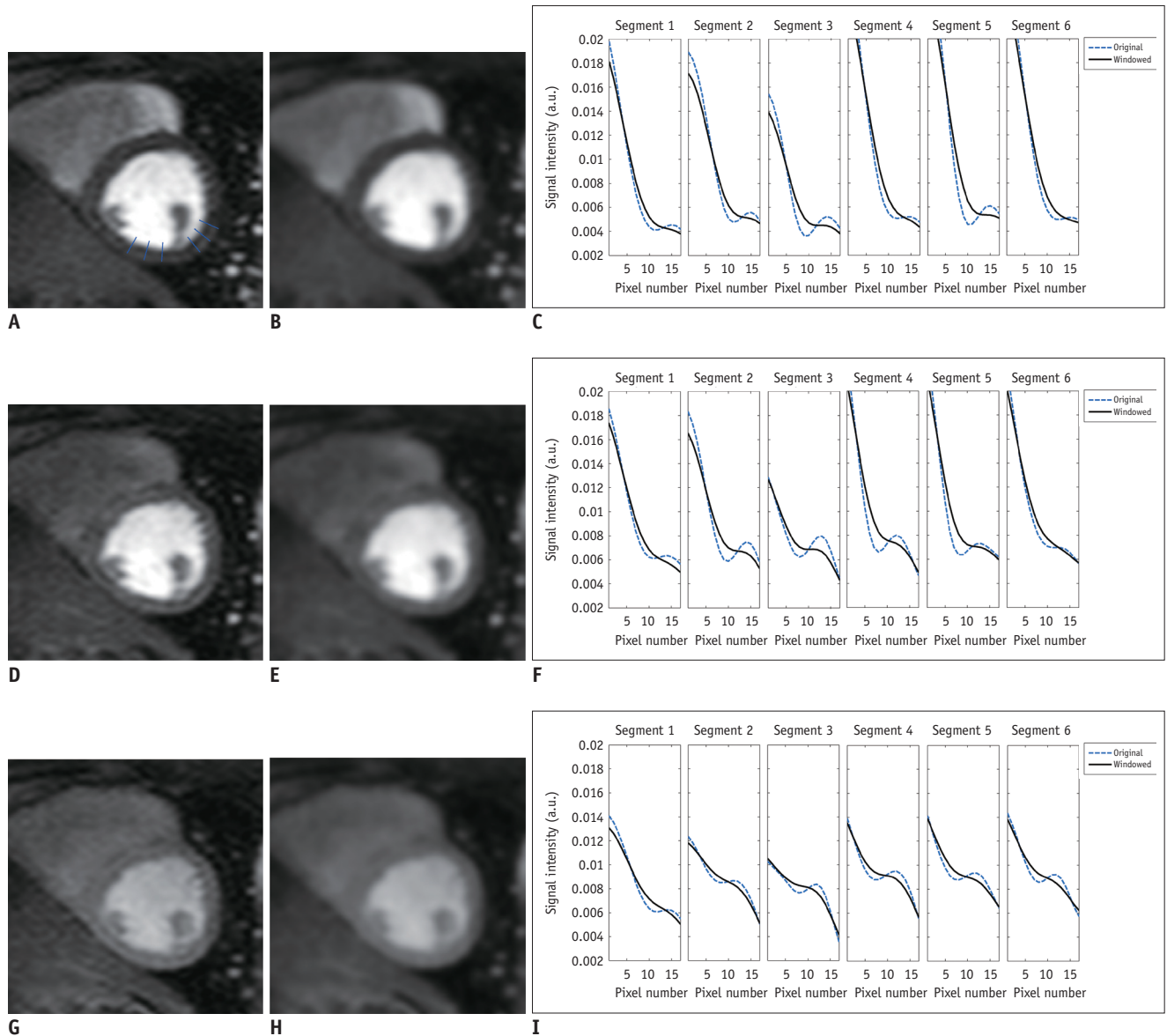


Fig. 4. Grayscale *in-vivo* perfusion images.

A, B, D, E, G, and **H** display *in-vivo* perfusion images at 9th (first row), 14th (second row), and 19th (third row) time frames following contrast agent injection in grayscale, before (1st column) and after (2nd column) k-space windowing. **C, F,** and **I** present intensity profiles along six transmural segments shown in **A**. After k-space windowing, quantitative signal dip in sub-endocardial layer was effectively suppressed, as confirmed by monotonic intensity changes. However, dark rim is still perceived across inferior and later walls, presumably due to Mach band illusion. Illusory dark rim is perceived more intensely at 9th and 14th time frames than at 19th frame, due to sharper intensity changes from LV to myocardium.

study, several transmural segments were manually selected and their intensity profiles were plotted over time. This approach, however, is not a practical solution to managing imaging artifacts, since the profile along a line of one-pixel thickness could be sensitive to noise and it would be time-consuming to specify multiple closely spaced segments to increase the analysis accuracy. Instead, it may be worthwhile to develop an image analysis tool which the user can use to specify a short azimuthal segment along

the LV-myocardium border and obtain an averaged intensity profile within the region of interest.

Another potential approach to identifying the illusory dark rim is to use the color scales with near-isoluminance for image display. Color scales with reduced luminance variation can remove the largest Mach band illusion, as shown by the two simple color maps used for confirming the illusory dark rim. However, human vision is less sensitive to contrast defined along color dimensions than along the

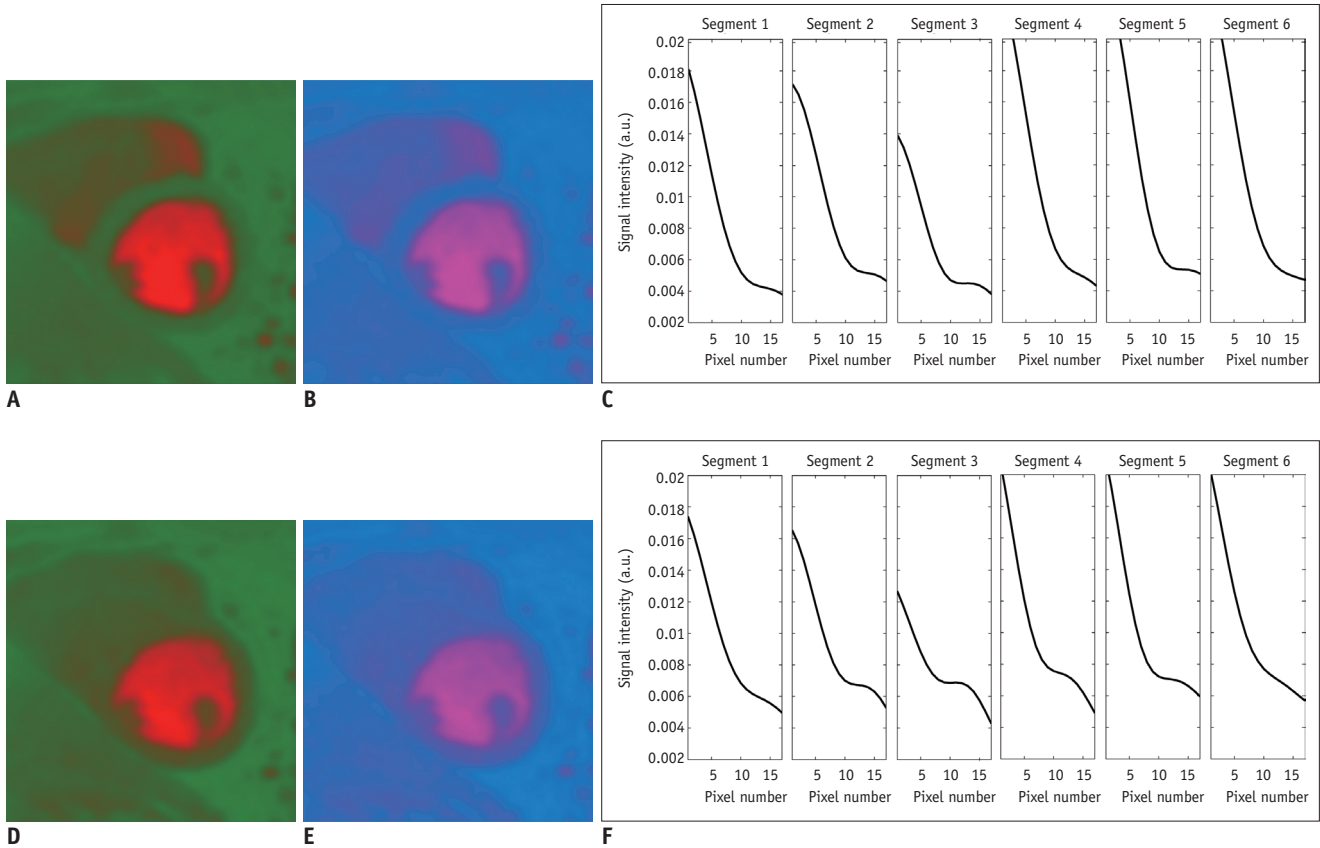


Fig. 5. Color displays of *in-vivo* perfusion images.

Color displays of same data as presented in Figure 4B (Fig. 5A, B; 9th time frame) and Figure 4E (Fig. 5D, E; 14th time frame) using two near-isoluminant color maps written as Equations [1] and [2]. Also shown are corresponding intensity profiles along six transmural segments (Fig. 5C, F). Illusory dark rim appears to be significantly reduced compared with Figure 4, due to reduced luminance variation in color scales. As trade-off, perceived spatial resolution is also reduced.

luminance dimension, which is used in the conventional gray scale (24). This will result in a reduction in perceived spatial resolution, possibly degrading the sensitivity of detecting true small defects. In general, a color map can be represented by a 1D trajectory in a three-dimensional (3D) color space defined by one luminance and two color dimensions. Finding the best trajectory that eliminates Mach band while retaining a high spatial resolution for human vision remains a worthwhile research question. Challenges in such optimization include the high degrees of freedom within the 3D search space, and possible individual differences in perceived spatial resolution and sensitivity to illusory dark rim. It should also be noted that the degree of dark rim perceived on color-coded images may vary between individuals, and the use of color maps should be considered a supplementary tool rather than an objective solution.

Dependence on Wall Location and Contrast Uptake

First-pass perfusion images typically contain two rapid

signal transitions (from LV to myocardium, and from myocardium to void background), each of which is similar to the linear ramp shown in Figure 1. The first transition from LV to myocardium produces an illusory dark rim in the inner layer of the myocardium, and the second transition produces an illusory bright rim in the outer layer of the myocardium. The adjacency of the two illusory rims renders the perceived endocardial dark rim stronger, possibly due to another form of visual illusion known as simultaneous contrast (25). The anterior and lateral walls appear to be more vulnerable to illusory DRA than other locations, since they border a void area. Conversely, when septal wall intensity happens to be similar to RV intensity (as in Fig. 2D), a small bright rim can be perceived in the epicardial layer, mitigating the perceived intensity of the endocardial dark rim.

The perceived intensity of the Mach band generally increases with the intensity difference across the transient ramp and the slope of the ramp (19). This property makes the strength of illusory DRA dependent on the timing of

contrast agent uptake in each compartment. For example, at peak myocardial enhancement (Figs. 2F, 3F), the intensity difference between LV and myocardium is relatively small, and the illusive DRA is weak compared to earlier time frames after peak LV enhancement. This implies a potential utility of evaluating the time course of the myocardial signal, which is available nowadays within most vendor-supplied or third-party cardiac analysis software. Since the signal-time curve wouldn't be affected by a visual illusion, simple display or calculation of the semi-quantitative index (such as the upslope) may serve as an additional solution for perceived DRA.

In conclusion, visual illusion is another potential cause of perceived DRA in contrast-enhanced MP MRI, as demonstrated by the perception of an illusory rim in the absence of an actual quantitative intensity undershoot. The perceived strength of DRA varies with time and spatial position within the myocardium during the first pass. These findings suggest the need for complementary ways to display images and quantitative plots of signal profiles, in addition to removing established sources of quantitative dark rim, such as Gibbs' ringing and cardiac motion.

Conflicts of Interest

The authors have no potential conflicts of interest to disclose.

Acknowledgments

Bosco S. Tjan who used to be a professor in the Psychology Department, University of Southern California, contributed to the manuscript significantly by explaining biological basis for human visual illusion. Very unfortunately however, he could not be listed as a co-author since he passed away by an incident.

ORCID iDs

Taehoon Shin

<https://orcid.org/0000-0003-1780-573X>

Krishna S. Nayak

<https://orcid.org/0000-0001-5735-3550>

REFERENCES

- Gerber BL, Raman SV, Nayak K, Epstein FH, Ferreira P, Axel L, et al. Myocardial first-pass perfusion cardiovascular magnetic resonance: history, theory, and current state of the art. *J Cardiovasc Magn Reson* 2008;10:18
- Jo Y, Kim J, Park CH, Lee JW, Hur JH, Yang DH, et al. Guideline for cardiovascular magnetic resonance imaging from the Korean Society of Cardiovascular Imaging-Part 1: standardized protocol. *Korean J Radiol* 2019;20:1313-1333
- Lee JW, Hur JH, Yang DH, Lee BY, Im DJ, Hong SJ, et al. Guidelines for cardiovascular magnetic resonance imaging from the Korean Society of Cardiovascular Imaging-Part 2: interpretation of cine, flow, and angiography data. *Korean J Radiol* 2019;20:1477-1490
- Wolff SD, Schwitter J, Coulden R, Friedrich MG, Bluemke DA, Biederman RW, et al. Myocardial first-pass perfusion magnetic resonance imaging: a multicenter dose-ranging study. *Circulation* 2004;110:732-737
- Plein S, Radjenovic A, Ridgway JP, Barmby D, Greenwood JP, Ball SG, et al. Coronary artery disease: myocardial perfusion MR imaging with sensitivity encoding versus conventional angiography. *Radiology* 2005;235:423-430
- Cheng AS, Pegg TJ, Karamitsos TD, Searle N, Jerosch-Herold M, Choudhury RP, et al. Cardiovascular magnetic resonance perfusion imaging at 3-tesla for the detection of coronary artery disease: a comparison with 1.5-tesla. *J Am Coll Cardiol* 2007;49:2440-2449
- Meyer C, Strach K, Thomas D, Litt H, Nöhle CP, Tiemann K, et al. High-resolution myocardial stress perfusion at 3 T in patients with suspected coronary artery disease. *Eur Radiol* 2008;18:226-233
- Gebker R, Jahnke C, Paetsch I, Kelle S, Schnackenburg B, Fleck E, et al. Diagnostic performance of myocardial perfusion MR at 3 T in patients with coronary artery disease. *Radiology* 2008;247:57-63
- Di Bella EV, Parker DL, Sinusas AJ. On the dark rim artifact in dynamic contrast-enhanced MRI myocardial perfusion studies. *Magn Reson Med* 2005;54:1295-1299
- Arai AE. Magnetic resonance first-pass myocardial perfusion imaging. *Top Magn Reson Imaging* 2000;11:383-398
- Plein S, Ryf S, Schwitter J, Radjenovic A, Boesiger P, Kozerke S. Dynamic contrast-enhanced myocardial perfusion MRI accelerated with k-t SENSE. *Magn Reson Med* 2007;58:777-785
- Storey P, Chen Q, Li W, Edelman RR, Prasad PV. Band artifacts due to bulk motion. *Magn Reson Med* 2002;48:1028-1036
- Zhao L, Saleno M, Kramer CM, Meyer CM. *The contribution of cardiac motion to dark rim artifacts in myocardial perfusion scans*. Proceeding of International Society for Magnetic Resonance in Medicine, 18th Annual Meeting;2010 May 1-7; Stockholm, Sweden
- Albert MS, Huang W, Lee JH, Patlak CS, Springer CS Jr. Susceptibility changes following bolus injections. *Magn Reson Med* 1993;29:700-708
- Schreiber WG, Schmitt M, Kalden P, Mohrs OK, Kreitner KF, Thelen M. Dynamic contrast-enhanced myocardial perfusion imaging using saturation-prepared TrueFISP. *J Magn Reson Imaging* 2002;16:641-652
- Ferreira P, Gatehouse P, Bucciarelli-Ducci C, Wage R, Firmin D. Measurement of myocardial frequency offsets during first pass

- of a gadolinium-based contrast agent in perfusion studies. *Magn Reson Med* 2008;60:860-870
17. Rodieck RW, Stone J. Analysis of receptive fields of cat retinal ganglion cells. *J Neurophysiol* 1965;28:833-849
18. Fiorentini A. *Mach band phenomena*. In: Alpern M, Aulhorn E, Barlow HB, Baumgardt E, Blackwell HR, Blough DS, et al., eds. *Handbook of sensory physiology, vol VII-4*. Berlin: Springer, 1972:188-201
19. Pessoa L. Mach bands: how many models are possible? Recent experimental findings and modeling attempts. *Vision Res* 1996;36:3205-3227
20. Pease PL. On color mach bands. *Vision Res* 1978;18:751-755
21. Ferreira P, Gatehouse P, Kellman P, Bucciarelli-Ducci C, Firmin D. Variability of myocardial perfusion dark rim Gibbs artifacts due to sub-pixel shifts. *J Cardiovasc Magn Reson* 2009;11:17
22. Strickland RN, Kim CS, McDonnell WF. *Luminance, hue, and saturation processing of digital color images*. SPIE conference on applications of digital image processing;1986 August 17; San Diego, CA, USA
23. Kellman P, Epstein FH, McVeigh ER. Adaptive sensitivity encoding incorporating temporal filtering (TSENSE). *Magn Reson Med* 2001;45:846-852
24. Williams D, Sekiguchi N, Brainard D. Color, contrast sensitivity, and the cone mosaic. *Proc Natl Acad Sci U S A* 1993;90:9770-9777
25. Palmer SE. *Vision science: photons to phenomenology*. Cambridge, MA: MIT Press, 1999